Model-free optimal trajectories in the image space

Youcef Mezouar, François Chaumette

Proceedings of the 2001 IEEE/RSJ
International Conference on Intelligent Robots and Systems
Maui, Hawaii, USA, Oct. 29 - Nov. 03, 2001

Model-Free Optimal Trajectories in the Image Space

Youcef Mezouar
Youcef.Mezouar@irisa.fr

François Chaumette
Francois.Chaumette@irisa.fr

IRISA - INRIA Rennes
Campus de Beaulieu,
35042 Rennes Cedex, France

Abstract

Since image-based servoing is a local control solution, it requires the definition of intermediate subgoals in the sensor space. This paper addresses the problem of generating realistic and optimal smooth trajectories of complex features in the image space. The model of the observed target and the internal camera parameters are assumed to be unknown. First a closed-form smooth collineation path between given starts and endpoints is obtained. This path is generated in order to correspond to an optimal camera path. The trajectories of the image features are then derived.

1 Introduction

Image-based servoing is now a well known local control framework [5], [7]. In this approach, the reference image of the object corresponding to a desired position of the robot is acquired first (during an off-line step) and some image features are extracted. An error is directly measured in the image between the current image and the reference one. The robot motion is then controlled in order to minimize the error (using for example a gradient descent approach). Sometimes, and especially when the displacement to realize is large, image and camera trajectories induced by image-based gradient descent are neither physically valid nor optimal [1]. In this article, we address the problem of finding realistic image trajectories (i.e corresponding to physically valid camera motion) and corresponding to an optimal camera path with respect to minimum acceleration criterion. The obtained trajectories can be used to improve significantly the system behavior since a local control solution works properly for a trajectory following [9].

Only few papers deal with path planning in image space. In [6] a trajectory generator using a stereo system is proposed and applied to obstacle avoidance. An alignment task using intermediate views of the object synthesized by image morphing is presented in [12]. A path planning for a straight-line robot translation observed by a weakly calibrated stereo system is performed in [11]. In previous work [9], we have proposed a potential field-based path planning generator that determines the trajectories in the image of a set of points lying on an unknown target. However, none of them were dealing with optimality issues. In this paper, first a smooth and optimal collineation path is obtained. Then, smooth image features trajectories corresponding to an optimal camera trajectory are computed.

The paper is organized as follow. In Section 2, we recall some properties of the collineation matrix. In Section 3 and Section 4, the cases where the camera is displaced according to a pure rotational and a pure translational motion are studied. In Section 5, the general case is addressed. In Section 6, the optimal collineation path is used to perform the optimal path in the camera image of visual features. The results are given in Section 7.

2 The Collineation matrix

Consider two views of a scene observed by a camera. A 3-D point $\mathbf{X}$ with homogeneous coordinates $\mathbf{X} = [X\ Y\ Z\ 1]^T$ is projected under perspective projection to a point $\mathbf{x}$ in the first image (with homogeneous coordinates measured in pixel $\mathbf{x} = [x\ y\ 1]^T$) and to a point $\mathbf{x}^*$ in the second image (with homogeneous coordinates measured in pixel $\mathbf{x}^* = [x^*\ y^*\ 1]^T$). It is well known that there exists a projective homography matrix $\mathbf{G}$ related to a virtual plane Π, such that for all point $\mathbf{X}$ belonging to Π, $\mathbf{x} \propto \mathbf{G}\mathbf{x}^*$ [1]. The matrix $\mathbf{G}$, when $\mathbf{x}$ and $\mathbf{x}^*$ are expressed in pixels, is called the collineation matrix. From the knowledge of several matched points, lines or contours [3, 2], it is possible to estimate the collineation matrix. Assuming that the camera calibration is known, the Euclidean

[1] $\mathbf{x} \propto \mathbf{G}\mathbf{x}^* \Longleftrightarrow \alpha\mathbf{x} = \mathbf{G}\mathbf{x}^*$ where α is a scaling factor

0-7803-6612-3/01/$10.00©2001 IEEE

homography can be computed up to a scalar factor:[2]

$$\mathbf{H} \propto \mathbf{K}^{+}\mathbf{G}\mathbf{K} \tag{1}$$

where $\mathbf{K}$ is a non singular matrix containing the intrinsic parameters of the camera. The Euclidean homography can be decomposed into a rotation matrix and a rank 1 matrix [4]:

$$\mathbf{H} = \mathbf{R} + \frac{\mathbf{b}}{d^*}\mathbf{n}^{*T} \tag{2}$$

where $\mathbf{R}$ and $\mathbf{b}$ represent the rotation matrix and the translation vector between the current and the desired camera frames (denoted $\mathcal{F}$ and $\mathcal{F}^*$ respectively), $\mathbf{n}^*$ is the unitary normal to the virtual plane expressed in $\mathcal{F}^*$ and d^* is the distance from Π to the origin of $\mathcal{F}^*$ (see Figure 1). From $\mathbf{G}$ and $\mathbf{K}$, it is thus possible to determine the camera motion parameters (i.e the rotation $\mathbf{R}$ and the scaled translation $\mathbf{b}_{d^*} = \frac{\mathbf{b}}{d^*}$) and the normal vector $\mathbf{n}^*$. If the camera is not perfectly calibrated (i.e $\widehat{\mathbf{K}}$ is used instead of $\mathbf{K}$), then, the parameters which can be estimated are [8]:

$$\widehat{\mathbf{R}} = \delta\mathbf{K}\mathbf{R}\delta\mathbf{K}^{+} \tag{3}$$

$$\widehat{\mathbf{n}}^{*T} = \frac{\mathbf{n}^{*T}\delta\mathbf{K}^{+}}{\|\mathbf{n}^{*T}\delta\mathbf{K}^{+}\|} \tag{4}$$

$$\widehat{\mathbf{b}}_{d^*} = \|\mathbf{n}^{*T}\delta\mathbf{K}^{+}\|\delta\mathbf{K}\mathbf{b}_{d^*} \tag{5}$$

In the sequel we assume that given an initial image and a desired image of the scene, some image features (points, lines, contours) can be extracted and matched. From the extracted image features, the collineation matrix at time $t = 0$, $\mathbf{G}_0$, can be computed. Note also that, when the desired configuration is reached (at time $t = 1$) the collineation matrix is proportional to the identity matrix: $\mathbf{G}^* \propto \mathbf{I}_{3\times 3}$. In the next sections, we consider the problem of finding a smooth path of the collineation matrix between $\mathbf{G}_0$ and $\mathbf{G}^*$ corresponding to an optimal camera path with respect to criterion which will be specified in the sequel.

3 Pure Rotational motion

In this section, we address the problem of finding an optimal closed form smooth path of the collineation when the collineation is a matrix similar (up to a scalar factor) to a rotation matrix, that is:

$$\mathbf{G} \propto \mathbf{K}\mathbf{R}\mathbf{K}^{+} \tag{6}$$

We begin with a brief review of necessary background on the Special Orthogonal group $SO(3)$.

[2] $\mathbf{K}^{+}$ denotes the inverse of $\mathbf{K}$

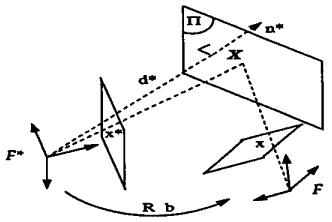

Figure 1: Geometry of two views

3.1 Brief Review of $SO(3)$

The group $SO(3)$ is the set of all 3×3 real orthogonal matrices with unit determinant and it has the structure of a Lie group. On a Lie group, the space tangent to the identity has the structure of a Lie algebra. The Lie algebra of $SO(3)$ is denoted by $so(3)$. It consists of the 3×3 skew-symmetric matrices, so that the elements of $so(3)$ are matrices of the form:

$$[\mathbf{r}] = \begin{bmatrix} 0 & -r_3 & r_2 \\ r_3 & 0 & -r_1 \\ -r_2 & r_1 & 0 \end{bmatrix}$$

One of the main connections between a Lie group and its Lie algebra is the exponential mapping. For every $\mathbf{R} \in SO(3)$, there exists at least one $[\mathbf{r}] \in so(3)$ such that $e^{[\mathbf{r}]} = \mathbf{R}$ with (Rodriguez formula):

$$\mathbf{R} = e^{[\mathbf{r}]} = \mathbf{I} + \frac{\sin\|\mathbf{r}\|}{\|\mathbf{r}\|}[\mathbf{r}] + \frac{1-\cos\|\mathbf{r}\|}{\|\mathbf{r}\|^2}[\mathbf{r}]^2 \tag{7}$$

where $\|\mathbf{r}\|$ is the standard Euclidean norm. Conversely, if $\mathbf{R} \in SO(3)$ such that $\text{Trace}(\mathbf{R}) \neq -1$ then:

$$[\mathbf{r}] = \log(\mathbf{R}) = \frac{\phi}{2\sin\phi}(\mathbf{R} - \mathbf{R}^T) \tag{8}$$

where ϕ satisfies:

$$\phi = \|\mathbf{r}\| = \arccos\left(\frac{1}{2}(\text{Trace}(\mathbf{R}) - 1)\right) \tag{9}$$

If $\text{Trace}(\mathbf{R}) = -1$, $\log(\mathbf{R})$ can be obtained noticing that $\mathbf{r} = \pm\pi\mathbf{u}$ where $\mathbf{u}$ is a unit length eigenvector of $\mathbf{R}$ associated with the eigenvalue 1.
Another important connection between $so(3)$ and $SO(3)$ involves angular velocities. If $\mathbf{R}(t)$ is a curve in $SO(3)$, then $\dot{\mathbf{R}}\mathbf{R}^T$ and $\mathbf{R}^T\dot{\mathbf{R}}$ are skew-symmetric, and hence element of $so(3)$. The element $\mathbf{w}$ of $so(3)$ such that:

$$[\mathbf{w}] = \mathbf{R}^T\dot{\mathbf{R}} \tag{10}$$

corresponds to the angular velocity of the rigid body.

3.2 Optimal collineation trajectories

We consider the problem **PR** of finding a path of the collineation corresponding to the minimum acceleration problem, that is:

$$\text{Find} \quad \mathbf{G}(t) \quad \text{minimizing} \quad J_1 = \int_0^1 \dot{\mathbf{w}}\dot{\mathbf{w}}^T dt$$

subject to $[\mathbf{w}] = \mathbf{R}^T\dot{\mathbf{R}}$, $\mathbf{G} \propto \mathbf{KRK}^+$ and with boundary conditions $\mathbf{G}(0) = \mathbf{G}_0$, $\mathbf{G}(1) = \mathbf{I}_{3\times3}$, $\mathbf{w}(0) = \mathbf{0}$ and $\mathbf{w}(1) = \mathbf{0}$.

Let us note that the boundary conditions of **PR** are verified if $\mathbf{R}(0) = \mathbf{R}_0$, $\mathbf{R}(1) = \mathbf{I}_{3\times3}$, $\mathbf{w}(0) = \mathbf{0}$ and $\mathbf{w}(1) = \mathbf{0}$ **(rotational problem)**. Note also that the considered boundary conditions are particularly important since they are indeed the desired boundary conditions in visual servoing applications.
The solution of **PR** and a nice property of the solution are given by the following proposition.

Proposition 1: The optimal path of the collineation matrix is given by:

$$\mathbf{G}(t) \propto \mathbf{G}_0\mathbf{\Gamma}(\mathbf{g}_0, q(t)) \tag{11}$$

where $q(t) = -2t^3 + 3t^2$ and:

$$\mathbf{\Gamma} = \mathbf{I} + \frac{\sin(\|\mathbf{g}_0\|q(t))}{\|\mathbf{g}_0\|}\{\mathbf{g}_0\} + \frac{1-\cos(\|\mathbf{g}_0\|q(t))}{\|\mathbf{g}_0\|^2}\{\mathbf{g}_0\}^2 \tag{12}$$

with:

$$\phi = \|\mathbf{g}_0\| = \text{Arcos}\left(\frac{1}{2}D_0^{-1/3}T_0 - 1\right) \tag{13}$$

$$\{\mathbf{g}_0\} = \frac{\|\mathbf{g}_0\|}{2\sin\|\mathbf{g}_0\|}\left(D_0^{1/3}\mathbf{G}_0^+ - D_0^{-1/3}\mathbf{G}_0\right) \tag{14}$$

where $D_0 = \det(\mathbf{G}_0)$, $T_0 = \text{Trace}(\mathbf{G}_0)$.

The collineation path given by (11) is independent of the internal camera parameters.

Proof: The solution of the rotational problem is given by [10]:

$$\mathbf{R}(t) = \mathbf{R}_0 e^{[\mathbf{r}_0]q(t)} \tag{15}$$

where $[\mathbf{r}_0] = \log(\mathbf{R}_0^T)$ and $q(t) = -2t^3 + 3t^2$. In the case of a pure rotational motion, it is easy to show from (6) that:

$$\begin{aligned} \mathbf{KRK}^+ &= D^{-1/3}\mathbf{G} \\ \text{Trace}(\mathbf{R}) &= D^{-1/3}T \end{aligned} \tag{16}$$

where $D = \det(\mathbf{G})$ and $T = \text{Trace}(\mathbf{G})$. According to (6) and (15) we have:

$$\mathbf{G}(t) \propto \mathbf{KR}_0 e^{[\mathbf{r}_0]q(t)}\mathbf{K}^+ = \mathbf{KR}_0\mathbf{K}^+\mathbf{K}e^{[\mathbf{r}_0]q(t)}\mathbf{K}^+$$

This equation can be rewritten as $\mathbf{G}(t) \propto \mathbf{G}_0\mathbf{\Gamma}$, where $\mathbf{\Gamma} = \mathbf{K}e^{[\mathbf{r}_0]q(t)}\mathbf{K}^+$ and according to (7), we obtain:

$$\mathbf{\Gamma} = \mathbf{I} + \frac{\sin(\|\mathbf{r}_0\|q(t))}{\|\mathbf{r}_0\|}\mathbf{K}[\mathbf{r}_0]\mathbf{K}^+ + \frac{1-\cos(\|\mathbf{r}_0\|q(t))}{\|\mathbf{r}_0\|^2}\mathbf{K}[\mathbf{r}_0]^2\mathbf{K}^+$$

With $\|\mathbf{g}_0\| = \|\mathbf{r}_0\|$ and $\{\mathbf{g}_0\} = \mathbf{K}[\mathbf{r}_0]\mathbf{K}^+$, the previous equation can be rewritten as (12), and (see (8)):

$$\{\mathbf{g}_0\} = \mathbf{K}\log(\mathbf{R}_0^T)\mathbf{K}^+ = \frac{\|\mathbf{g}_0\|}{2\sin\|\mathbf{g}_0\|}(\mathbf{KR}_0^T\mathbf{K}^+ - \mathbf{KR}_0\mathbf{K}^+).$$

By introducing (16) in the previous equation, we obtain (14). Finally, using (9) and (16), we deduce (13). The initial value of the collineation $\mathbf{G}_0$ is not affected by errors on intrinsic parameters since it is extracted directly from image data. According to (11), (12), (13) and (14), the collineation path given by (11) is thus independent of the camera parameters.

Remark: The path given by the proposition 1 corresponds to a shortest distance path of the rotation matrix (minimal geodesic) with respect to an adequately chosen Riemannian metric on $SO(3)$.
In the next subsection, the case of a pure translational camera motion is studied.

4 Pure translational motion

If the camera motion is a pure translation, the collineation matrix has the following particular form:

$$\mathbf{G} \propto \mathbf{I} + \mathbf{Kb}_{d^*}\mathbf{n}^{*T}\mathbf{K}^+ \tag{17}$$

In this section, we address the problem (**PT**) of finding the path of the collineation matrix when it is given by (17) and corresponding to the minimum acceleration problem, that is:

$$\text{Find} \quad \mathbf{G}(t) \quad \text{minimizing} \quad J_2 = \int_0^1 \dot{\mathbf{v}}^T\dot{\mathbf{v}}dt$$

where $\mathbf{v}$ denotes the time derivative of $\mathbf{b}$, subject to (17), with boundary conditions $\mathbf{G}(0) \propto \mathbf{G}_0$, $\mathbf{G}(1) \propto \mathbf{I}$, $\mathbf{v}(0) = \mathbf{v}(1) = \mathbf{0}$.
Note once again that the boundary conditions of **PT** are verified if $\mathbf{b}(0) = \mathbf{b}_0$, $\mathbf{b}(1) = \mathbf{0}$ and $\mathbf{v}(0) = \mathbf{v}(1) = \mathbf{0}$ **(translational problem)**. The considered boundary conditions are indeed the desired boundary conditions in the context of visual servoing.

proposition 2: The optimal path of the collineation matrix in the sense of **PT** is given by:

$$\mathbf{G}(t) \propto q(t)\mathbf{I} + \frac{(1-q(t))}{\alpha_0}\mathbf{G}_0 \tag{18}$$

where α_0 is a real solution of the equation:

$$2\alpha^3 - T_0\alpha^2 + D_0 = 0 \tag{19}$$

and *the optimal smooth trajectories given by (18) is not affected by error on intrinsic parameters.*

proof: The solutions of the translational problem is given by:

$$\mathbf{b}(t) = (1 - q(t))\mathbf{b}_0 \tag{20}$$

By introducing (20) in (17), we obtain:

$$\begin{aligned} \mathbf{G}(t) &\propto \mathbf{I} + \mathbf{K}(1 - q(t))\mathbf{b}_{d^*0}\mathbf{n}^{*T}\mathbf{K}^+ \\ &\propto q(t)\mathbf{I} + (1 - q(t))(\mathbf{I} + \mathbf{K}\mathbf{b}_{d^*0}\mathbf{n}^{*T}\mathbf{K}^+) \end{aligned}$$

and noticing that $\mathbf{G}_0 = \alpha_0(\mathbf{I} + \mathbf{K}\mathbf{b}_{d^*0}\mathbf{n}^{*T}\mathbf{K}^+)$, we deduce (18). From (17), we easily obtain:

$$\begin{cases} Trace(G_0) = T_0 = \alpha_0(3 + \mathbf{b}_{d^*0}^T\mathbf{n}) \\ Det(G_0) = D_0 = \alpha_0^3(1 + \mathbf{b}_{d^*0}^T\mathbf{n}) \end{cases}$$

and by combining the previous equations, we deduce that α_0 is a solution of (19).
The path of the collineation matrix given by (18) is independent of the **K**-matrix since the initial value of the collineation matrix $\mathbf{G}_0$ and thus α_0 (refer to (19)) are independent of the camera intrinsic parameters.

Remark: The path given by (18) corresponds to a shortest distance path in $\Re^3$ (straight line) between the initial and desired camera positions.

5 General camera motions

We assume now that the initial camera frame $\mathcal{F}^i$ is displaced by the matrix:

$$\mathbf{D}(t) = \begin{bmatrix} \mathbf{R}(t) & \mathbf{b}(t) \\ \mathbf{0} & 1 \end{bmatrix}$$

to the desired camera frame $\mathcal{F}^*$. In this case the collineation matrix is given by $\mathbf{G}(t) \propto \mathbf{K}^+\left(\mathbf{R} + \mathbf{b}_{d^*}\mathbf{n}^{*T}\right)\mathbf{K}$. We denote $\mathbf{U}$ the 6×1 vector $[\mathbf{v}^T\mathbf{w}^T]^T$. We address now the following problem (**PC**):

$$\text{Find} \quad \mathbf{G}(t) \quad \text{minimizing} \quad J_3 = \int_0^1 \dot{\mathbf{U}}^T\dot{\mathbf{U}}dt$$

subject to (10), $\mathbf{v} = \dot{\mathbf{b}}$ and with boundary conditions: $\mathbf{G}(0) \propto \mathbf{G}_0$, $\mathbf{G}(1) \propto \mathbf{I}_{3\times3}$, $\mathbf{U}(0) = \mathbf{U}(1) = \mathbf{0}_{6\times1}$. The boundary conditions are verified if $\mathbf{R}(0) = \mathbf{R}_0$, $\mathbf{b}(0) = \mathbf{b}_0$, $\mathbf{R}(1) = \mathbf{I}$ and $\mathbf{b}(1) = \mathbf{0}$ (**rigid motion problem**). Once again, the considered boundary conditions are particularly important since they are the desired boundary conditions in the context of visual servoing.
The solution of **PC** and a result about its dependence on camera calibration are given by the following proposition.

Proposition 3: The optimal path of the collineation matrix in the sense of **PC** is given by:

$$\mathbf{G}(t) \propto (1 - q(t))\mathbf{\Phi}_0 + (\mathbf{G}_0 + \mathbf{\Phi}_0)\mathbf{\Gamma}(\mathbf{r}_0, t) \tag{21}$$

where:

$$\begin{cases} \mathbf{\Gamma}(\mathbf{r}_0, q(t)) = \mathbf{K}\mathbf{e}^{[\mathbf{r}_0]q(t)}\mathbf{K}^+ \\ \mathbf{\Phi}_0 = \mathbf{K}\mathbf{b}_{0d^*}\mathbf{n}^{*T}\mathbf{K}^+ \end{cases} \tag{22}$$

Assuming (3), (4) and (5), the path given by (22) is not affected by error on intrinsic error.

proof: The solution of the rigid motion problem is given by:

$$\begin{cases} \mathbf{b}(t) = (1 - q(t))\mathbf{b}_0 \\ \mathbf{R}(t) = \mathbf{R}_0\mathbf{e}^{[\mathbf{r}_0]q(t)} \end{cases}$$

According to (1) and (2), the corresponding collineation path is given by:

$$\mathbf{G}(t) \propto \mathbf{K}(\mathbf{R}_0\mathbf{e}^{[\mathbf{r}_0]q(t)} + (1 - q(t))\mathbf{b}_{0d^*}\mathbf{n}^{*T})\mathbf{K}^+$$

This path is equivalent to the path given by :

$$\begin{aligned} \mathbf{G}(t) \propto \; & \mathbf{K}\left(\mathbf{R}_0\mathbf{e}^{[\mathbf{r}_0]q(t)} + (1 - q(t))\mathbf{b}_{0d^*}\mathbf{n}^{*T} + \right. \\ & \left. \mathbf{b}_{0d^*}\mathbf{n}^{*T}\mathbf{e}^{[\mathbf{r}_0]q(t)} - \mathbf{b}_{0d^*}\mathbf{n}^{*T}\mathbf{e}^{[\mathbf{r}_0]q(t)}\right)\mathbf{K}^+ \end{aligned}$$

and can be rewritten as (21). We note that the matrix of camera internal parameters appears explicitly in the path given by (21). The initial collineation matrix $\mathbf{G}_0$ is not affected by error on intrinsic parameters since it is directly computed from image data. Assume now that the non-singular matrix $\widehat{\mathbf{K}}$ is used instead of $\mathbf{K}$, we have:

$$\begin{cases} \widehat{\mathbf{\Phi}}_0 = \widehat{\mathbf{K}}\widehat{\mathbf{b}}_{0d^*}\widehat{\mathbf{n}}^{*T}\widehat{\mathbf{K}}^+ \\ \widehat{\mathbf{\Gamma}}(\mathbf{r}_0, q(t)) = \widehat{\mathbf{K}}\mathbf{e}^{[\widehat{\mathbf{r}}_0]q(t)}\widehat{\mathbf{K}}^+ \end{cases}$$

By introducing (4) and (5) in $\widehat{\mathbf{\Phi}}_0$, we obtain:

$$\begin{aligned} \widehat{\mathbf{\Phi}}_0 &= \widehat{\mathbf{K}}\|\mathbf{n}^{*T}\delta\mathbf{K}^+\|\delta\mathbf{K}\mathbf{b}_{d^*}\frac{\mathbf{n}^{*T}\delta\mathbf{K}^+}{\|\mathbf{n}^{*T}\delta\mathbf{K}^+\|}\mathbf{K}^+ \\ &= \mathbf{K}\mathbf{b}_{0d^*}\mathbf{n}^{*T}\mathbf{K}^+ = \mathbf{\Phi}_0 \end{aligned}$$

Furthermore (refer to (8)):

$$[\widehat{\mathbf{r}}_0] = \frac{\widehat{\phi}}{2sin(\widehat{\phi})}(\widehat{\mathbf{R}}_0^T - \widehat{\mathbf{R}}_0) = \widehat{\beta}(\widehat{\mathbf{R}}_0^T - \widehat{\mathbf{R}}_0) \tag{23}$$

where $\widehat{\beta} = \frac{\widehat{\phi}}{2sin\widehat{\phi}}$ and $\widehat{\phi}$ satisfies $1+2cos\widehat{\phi} = \text{Trace}(\widehat{\mathbf{R}}_0)$. Since $\widehat{\mathbf{R}}_0$ is similar to $\mathbf{R}_0$ (see (3)), $\text{Trace}(\widehat{\mathbf{R}}_0) = \text{Trace}(\mathbf{R}_0)$ and thus $\widehat{\phi} = \phi$ and $\widehat{\beta} = \beta$. By injecting (23) in (7), we obtain :

$$\widehat{\mathbf{\Gamma}}(\mathbf{r}_0, q(t)) = \widehat{\mathbf{K}}(\mathbf{I} + \beta\frac{sin(\|\mathbf{r}_0\|q(t))}{\|\mathbf{r}_0\|}(\widehat{\mathbf{R}}_0^T - \widehat{\mathbf{R}}_0) + \beta^2\frac{1-cos(\|\mathbf{r}_0\|q(t))}{\|\mathbf{r}_0\|^2}(\widehat{\mathbf{R}}_0^T - \widehat{\mathbf{R}}_0)^2)\widehat{\mathbf{K}}^+$$

and noticing that $\widehat{\mathbf{K}}\widehat{\mathbf{R}}_0\widehat{\mathbf{K}}^+ = \mathbf{K}\mathbf{R}_0\mathbf{K}^+$, we finally obtain $\widehat{\mathbf{\Gamma}}(\widehat{\mathbf{r}}_0, q(t)) = \mathbf{\Gamma}(\mathbf{r}_0, q(t))$. Thus, the collineation trajectory given by (21) is independent of the choice of the non singular matrix $\widehat{\mathbf{K}}$.

6 Features trajectories in the image

In order to control efficiently a robot using visual information, we have to perform the trajectories of some image features in the image space. More precisely, we want to perform a smooth trajectories $\mathbf{s}^*(t) = [x_1^*(t)\ y_1^*(t)\ \cdots\ x_n^*(t)\ y_n^*(t)]^T$ of n projected points in the image between a given start point $\mathbf{s}^*(0) = [x_1^*(0)\ y_1^*(0)\ \cdots\ x_n^*(0)\ y_n^*(0)]^T$ and a given desired point $\mathbf{s}_f = \mathbf{s}^*(1) = [x_{f1}\ y_{f1}\ \cdots\ x_{fn}\ y_{fn}]^T$. We denote $\mathbf{x}_i^*(t) = [x_i^*(t)\ y_i^*(t)\ 1]^T$ and $\mathbf{x}_{fi} = [x_{fi}\ y_{fi}\ 1]^T$ the vectors of homogeneous coordinates expressed in pixel of the projection of a 3-D point $\mathcal{M}_i$ in the current desired (at time t) and final desired (at time $t = 1$) images. It is well known that:

$$\mathbf{h}_i(t) = \alpha_i(t)\mathbf{x}_i^*(t) = \mathbf{G}(t)\mathbf{x}_{fi} + \beta_i\mathbf{e}(t) \qquad (24)$$

where $\alpha_i(t)$ is a positive scaling factor depending on time, β_i is a constant scaling factor null if the target point belongs to Π and $\mathbf{e}(t) = \mathbf{K}\mathbf{b}(t)$ represents the epipole. After that the initial collineation has been estimated, the optimal path of the collineation matrix can be computed as previously described. The initial value of the epipole, $\mathbf{e}(0) = \mathbf{e}_0$, can also be computed directly from image data (i.e, $\mathbf{e}_0$ is independent of the $\mathbf{K}$-matrix). Furthermore, it is easy to show (from (20)) that the optimal trajectories of the epipole, with respect to the previously cited criteria, are of the form:

$$\mathbf{e}(t) = (1 - q(t))\mathbf{e}_0 \qquad (25)$$

Such trajectories of the epipole are not affected by error on intrinsic parameters. Note also that the scaling factor β_i is not time dependent and can be computed directly from the initial and desired image data [3]:

$$\beta_i = sign\left(-\frac{[\mathbf{G}_0\mathbf{x}_{fi} \wedge \mathbf{x}_i^*(0)]_1}{[\mathbf{e}_0 \wedge \mathbf{x}_i^*(0)]_1}\right)\frac{\|\mathbf{G}_0\mathbf{x}_{fi} \wedge \mathbf{x}_i^*(0)\|}{\|\mathbf{e}_0 \wedge \mathbf{x}_i^*(0)\|} \qquad (26)$$

[3] $\mathbf{v}_j$ denotes the j^{th} components of $\mathbf{v}$

The vector $\mathbf{h}_i$ is not affected by error on intrinsic parameters since $\mathbf{G}(t)$, $\mathbf{e}(t)$ and β_i (for $i \in 1\cdots n$) can be computed without error even if the $\mathbf{K}$-matrix is unknown. The trajectories of the considered point in the image corresponding to an optimal camera path can thus also be computed without error, with:

$$x_i^*(t) = \frac{[\mathbf{h}_i(t)]_1}{[\mathbf{h}_i(t)]_3} \quad y_i^*(t) = \frac{[\mathbf{h}_i(t)]_2}{[\mathbf{h}_i(t)]_3} \qquad (27)$$

7 Results

Experiments were performed with images acquired by an eye-in-hand robotic platform. The intrinsic parameters ($\mathbf{K}$-matrix) given by the camera manufacturer are used. The camera displacement between the acquisition of initial and desired images (boxed in Figure 3) is a rigid motion. The initial collineation matrix is:

$$\mathbf{G}_0 = \begin{bmatrix} 0.4603 & 0.4145 & -597.3284 \\ -0.2476 & 0.6107 & -376.0835 \\ -0.0001 & 0.0006 & -1.5281 \end{bmatrix}$$

Intermediate images synthesized (at time $t = k \times 0.1$ with $k \in \{1\cdots 8\}$) using the equation (27) and the solution of the problem **PC** are given in Figure 3. The corresponding camera trajectory is plotted in Figure 2.

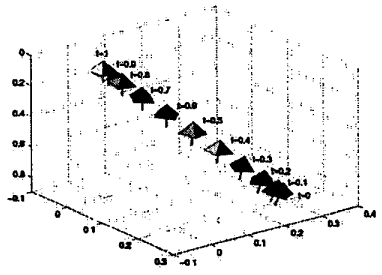

Figure 2: Camera trajectory

8 Conclusion

In this paper, we have addressed the problem of finding the trajectories in the image space of image features corresponding to the camera minimum acceleration. The obtained camera trajectory corresponds to a minimum geodesic in $SE(3)$. The method is model-free and the uncalibred cases has been studied. Future work will be devoted to introduce constraints in order to keep the target in the camera field of view or to avoid the robot joint limits.

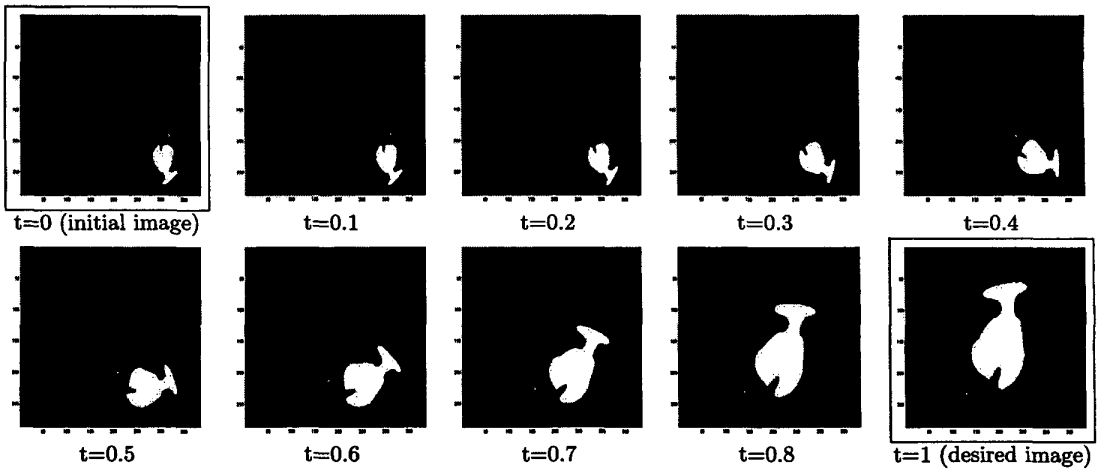

Figure 3: Image trajectories

References

[1] F. Chaumette. Potential problems of stability and convergence in image-based and position-based visual servoing. *The Confluence of Vision and Control, D. Kriegman, G. Hager, A. Morse (eds), LNCIS Series, Springer Verlag*, 237:66–78, 1998.

[2] G. Chesi, E. Malis, and R. Cipolla. Automatic segmentation and matching of planar contours for visual servoing. In *International Conference on Robotics and Automation*, San Francisco, April 2000.

[3] O. Faugeras. *Three-dimensionnal computer vision : a geometric view point.* MIT press, Cambridge, Massachusetts, 1993.

[4] O. Faugeras and F. Lustman. Motion and structure from motion in a piecewise planar environment. *Int. Journal of Pattern Recognition and Artificial Intelligence*, 2(3):485–508, 1988.

[5] K. Hashimoto. *Visual Servoing: Real Time Control of Robot Manipulators Based on Visual Sensory Feedback.* World Scientific Series in Robotics and Automated Systems, Vol 7,World Scientific Press, Singapor, 1993.

[6] K. Hosoda, K. Sakamoto, and M. Asada. Trajectory generation for obstacle avoidance of uncalibrated stereo visual servoing without 3d reconstruction. *IEEE/RSJ Int. Conf. on Intelligent Robots and Systems*, 1(3):29–34, August 1995.

[7] S. Hutchinson, G.D. Hager, and P.I. Corke. A tutorial on visual servo control. *IEEE Trans. on Robotics and Automation*, 12(5):651–670, October 1996.

[8] E. Malis and F. Chaumette. 2 1/2 d visual servoing with respect to unknown objects through a new estimation scheme of camera displacement. *Int. Journal of Computer Vision*, 37(1):79–97, June 2000.

[9] Y. Mezouar and F. Chaumette. Path planning in image space for robust visual servoing. In *IEEE Int. Conf. on Robotics and Automation*, volume 3, pages 2759–2764, San Francisco, April 2000.

[10] F. C Park and B. Ravani. Smooth invariant interpolation of rotations. *ACM Transactions on Graphics*, 16(3):277–295, July 1997.

[11] A. Ruf and R. Horaud. Visual trajectories from uncalibrated stereo. *IEEE Int. Conf. on Intelligent Robots and Systems*, pages 83–91, September 1997.

[12] R. Singh, R. M. Voyle, D. Littau, and N. P. Papanikolopoulos. Alignement of an eye-in-hand system to real objects using virtual images. *Workshop on Robust Vision for Vision-Based Control of Motion, IEEE Int. Conf. on Robotics and Automation*, May 1998.